Supplemental Figure 1

A

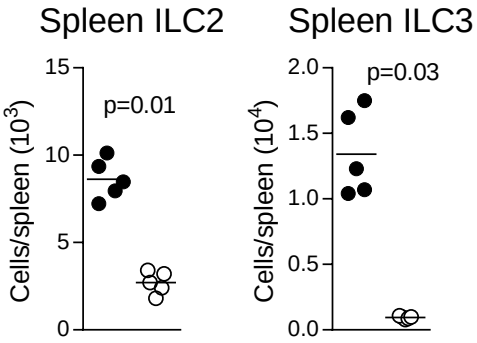

Supplemental Figure 1. Radiation sensitivity of ILCs in the spleen. (**A**) Quantitation of ILC2 and ILC3 cells in the spleen of B6D2 mice after lethal dose radiation, without irradiation (black dots) or 24 hours after receiving radiation (950cGy) (open circles) as analyzed by flow cytometry. These represent 3 independent experiments, bar graphs are average ± SEM, student's *t*-test with Welch's correction, n=5 for each group.

Supplemental Figure 2

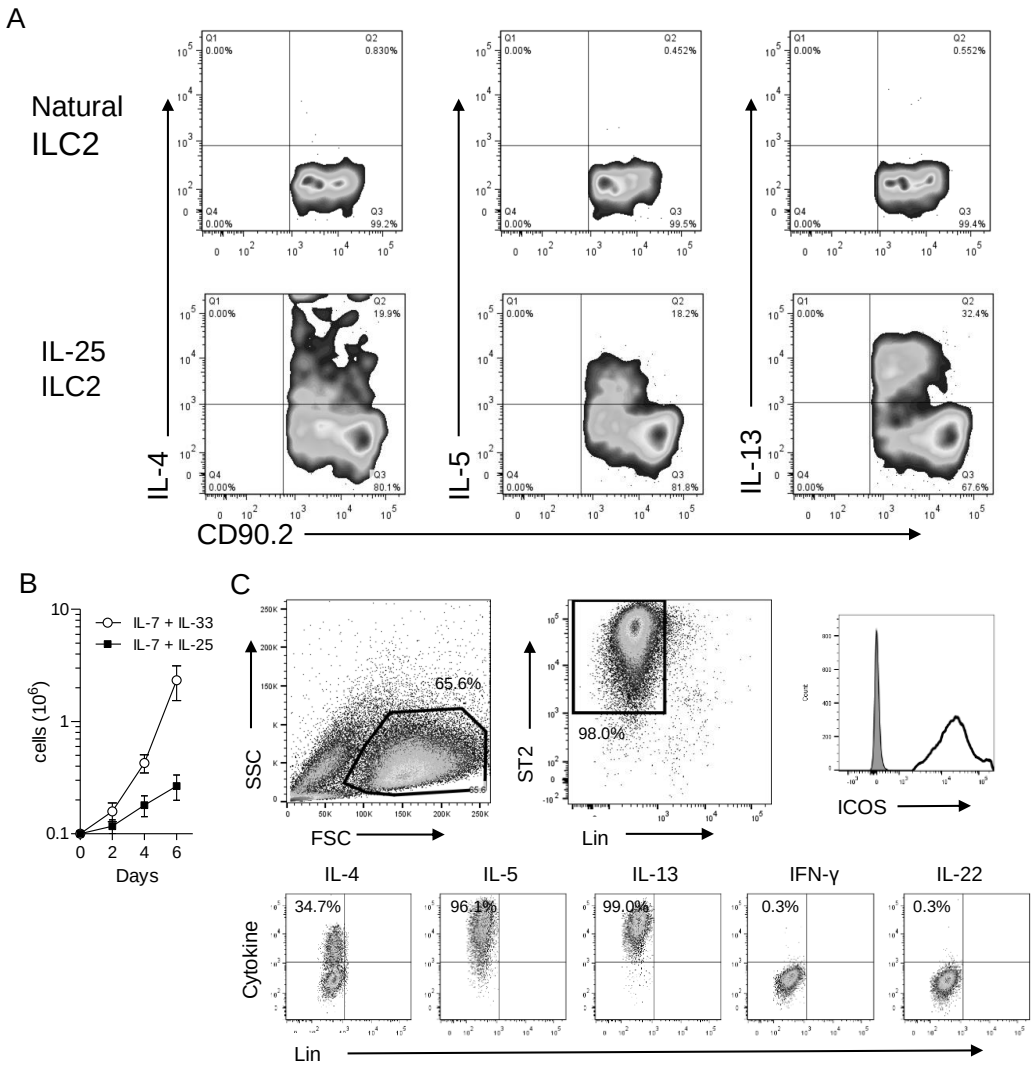

Supplemental Figure 2. ILC2s *in vitro* isolation and expansion. (**A**) IC staining of IL-4, IL-5 and IL-13 by ILC2s in the absence of IL-25 treatment and ILC2s after 4 days of IL-25 treatment, gated as $Lin^-/CD45^+/CD127^+$. Neill *et.al*. showed that after isolation, ILC2s could be expanded *in vitro* with IL-33 and IL-7 treatment (24). Using this approach, we found greater than a 10 fold expansion of ILC2s *in vitro* after 6 days compared to IL-25 treated cultures. (**B**) IL-33 and IL-7 treatment increases ILC2 proliferation *in vitro* compared to IL-25 with IL-7 (10ng/ml ea.), adjusted average cell number ± SEM. IL-33 and IL-7 treatment also activated ILC2s increasing the precentage of cultured cells that produced IL-4, IL-5 and IL-13 with no evidence of expansion of other ILC groups; IFN-γ in ILC1 cells or IL-22 in ILC3 cells. (**C**) Phenotype and cytokine expression of ILC2s after 6 days of *in vitro* expansion by IC staining and flow cytometry (Gating shown for FSC/SSC then $ST2^+/Lin^-$ cells). These represent 3 independent experiments.

Supplemental Figure 3

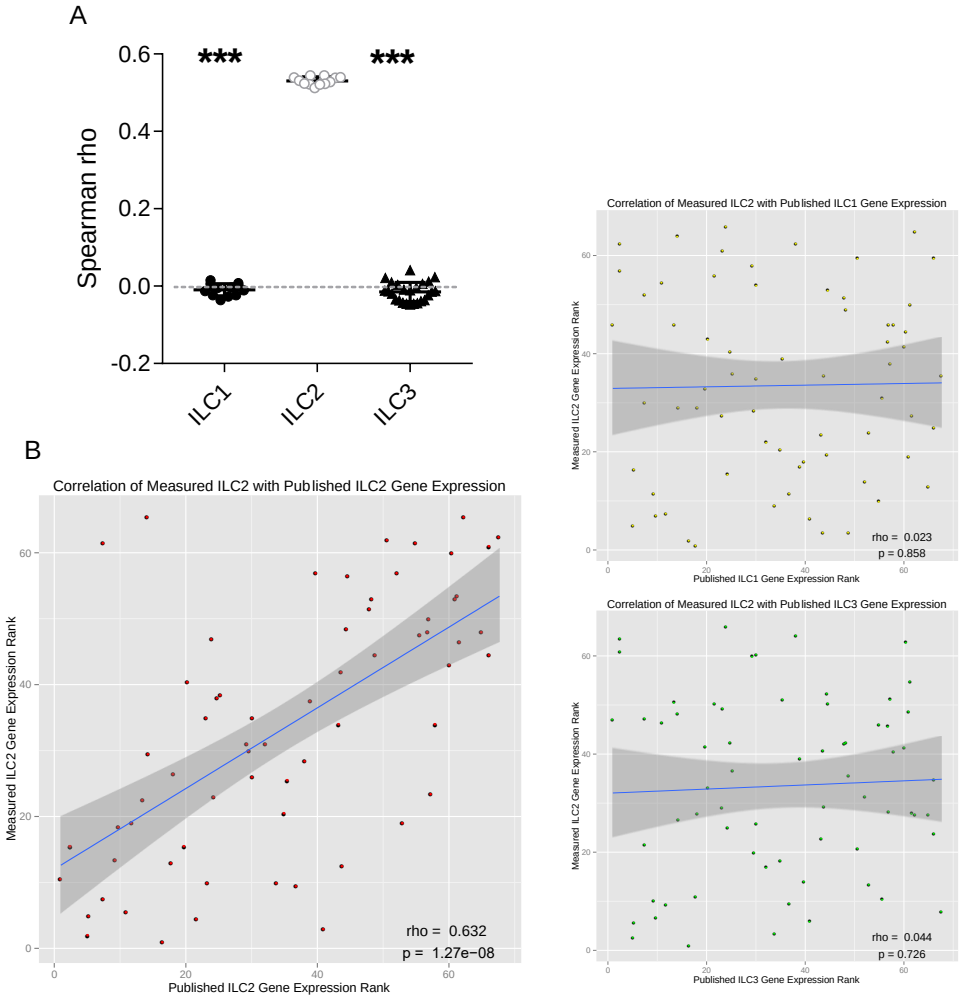

Supplemental Figure 3. ***In vitro*** **expanded ILC2 transcriptome phenotype.** To verify that *in vitro* expanded cells were ILC2s, we performed RNA-seq from our cultured cells and compared the phenotype to published gene expression values for each ILC subset (57). The cytokine and gene expression profiles of our cultured cells strongly correlated with the published profile of ILC2s isolated from LP with no correlation to ILC1 and/or ILC3 cells. (**A**) Spearman rank correlations between gene expression values of ILC-associated genes for measured ILC2 (n = 6) and published ILC1 (n = 2, 12 comparisons), ILC2 (n = 2, 12 comparisons), and ILC3 (n = 8, 48 comparisons) were calculated and used as a statistic. Significance between sample groups was evaluated using the Kruskal-Wallis test, $p<0.0001$. (**B**) Mean rank expression values for each gene from each published group were plotted against mean rank expression values in the cultured ILC2s. Right upper panel: Correlation with published ILC1s. Right lower panel: Correlation with published ILC3s. Left panel: Correlation with published ILC2s. Significance was tested using the 'cor.test' module in R (method = 'spearman'). Spearman rho values and p values of correlation significance are shown in the lower right.

Supplemental Figure 4

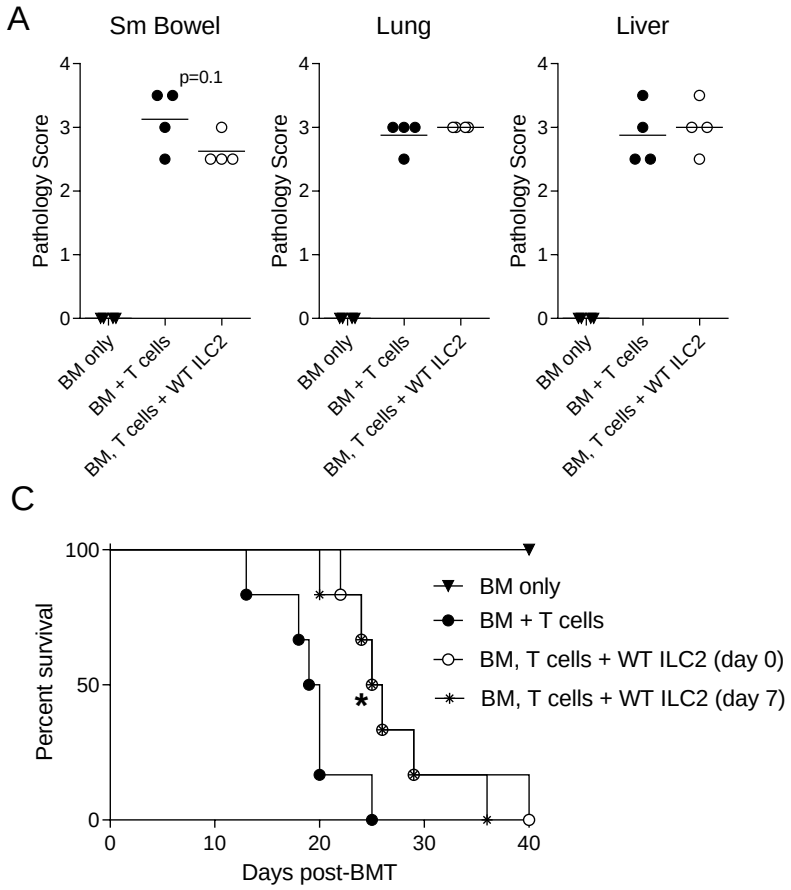

Supplemental Figure 4. Co-transplantation of donor ILC2s reduces aGvHD incidence. (**A**) Pathology scores of histological evaluations of GvHD target organs small bowel, lung and liver 20 days after BMT, as described in (Figure 2d), student's *t*-test with Welch's correction. (**B**) Clinical score of BALB/cJ recipients described in (Figure 2e), ** $p<0.01$ by 2 way ANOVA, with Bonferroni correction for repeated measures of multiple comparisons. (**C**) Kaplan-Meier plot of survival of BALB/cJ recipients that received BM alone (BM only), BM and B6 splenic T cells (BM + T cells) and WT ILC2s either at the time of transplant [BM, T cells + WT ILC2 (Day 0)] or 7 days after transplant [BM, B6 T cells + WT ILC2 (Day 7)], represents two experiments (n=6), * $p<0.05$ by Log-rank (Mantel-cox) test.

Supplemental Figure 5

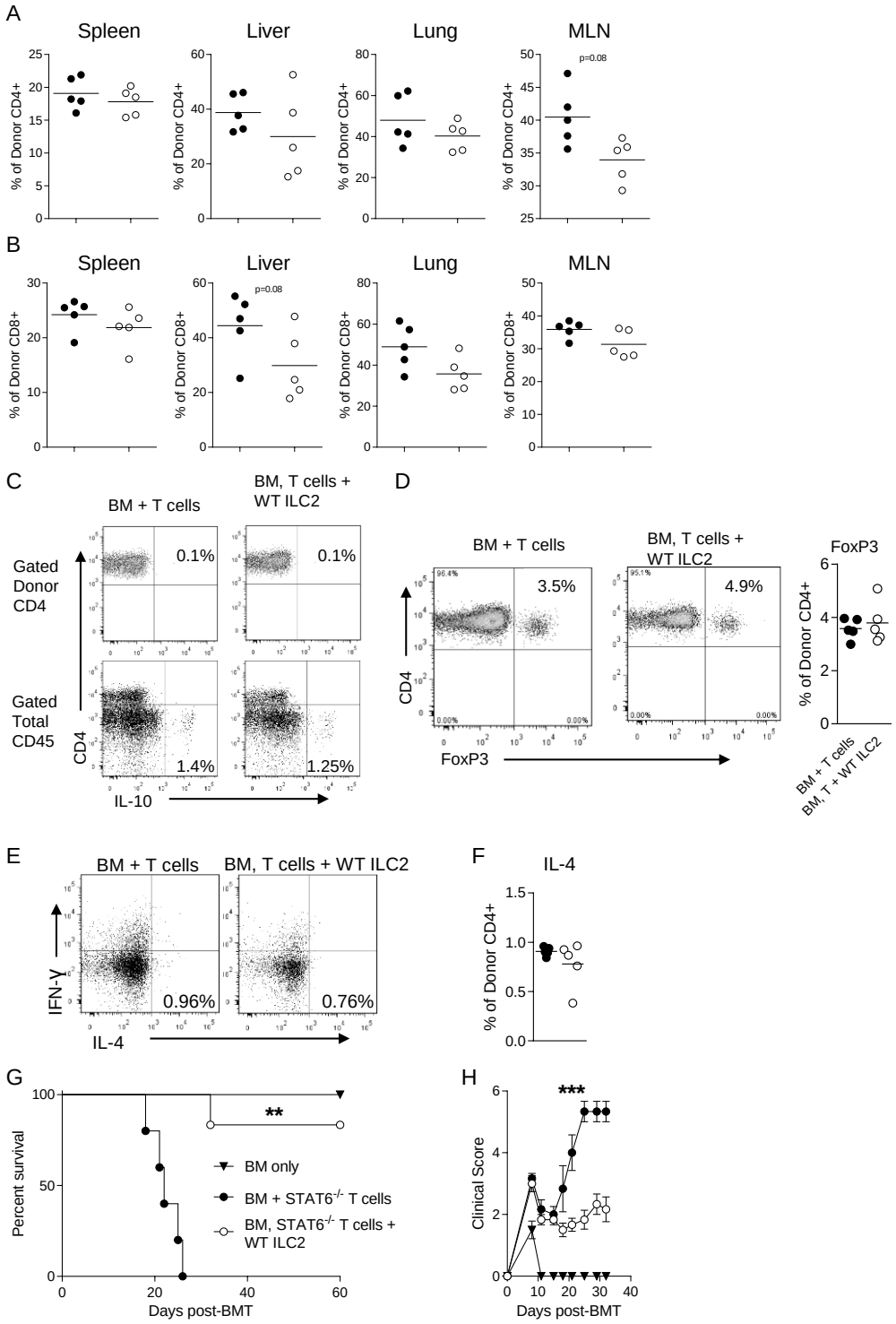

Supplemental Figure 5. T cell analysis following ILC2 co-transplantation. (**A**) Flow cytometry analysis of donor T cells in GvHD target organs 12 days post-transplant in (**A**) $CD4^+$ and (**B**) $CD8^+$ donor T cells, BM + T cells (black dots) or BM, T cells + WT ILC2 (open circles), average ± SEM, student's *t*-test with Welch's correction. Representative of two experiments, n=5. ILC2 suppression of aGvHD is independent of enhanced Th2 differentiation of donor T cells. Evaluation of donor T cell phenotype in colon LP 12 days after allo-SCT by

IC staining and flow cytometry (**C**) Dot plots of IL-10 producing $CD4^+$ donor T cells and total $CD45^+$ cells of allo-SCT recipients. (**D**) Flow cytometry plots of donor $CD4^+$ T cell expression of FoxP3 and bar graph, mean ± SEM, n=. (**E**) IL-4 expression was evaluated in donor T cells in the colon LP by intracellular staining and flow cytometry, representative dot plot shown. (**F**) Percentage of IL-4 expressing donor T cells, BM + T cells (black dots) or BM, T cells + WT ILC2 (open circles), mean ± SEM, represent two independent experiments, n=5. (**G**) Kaplan-Meier plot of survival of lethally irradiated B6D2 mice (950cGy) that received 3.0×10^6 B6 WT TCD BM (BM only), BM plus 4.0×10^6 total $STAT6^{-/-}$ splenic T cells (BM + $STAT6^{-/-}$ T cells) or BM plus $STAT6^{-/-}$ T cells with 4.0×10^6 B6 WT activated ILC2s (BM, $STAT6^{-/-}$ T cells + WT ILC2), one representative experiment shown (n=6 each), ** $p<0.01$ by Log-rank (Mantel-cox) test. (**H**) Clinical scores of recipients from survival study in (g), *** $p<0.001$ by 2-way ANOVA, with Bonferroni correction for repeated measures of multiple comparisons.

Supplemental Figure 6

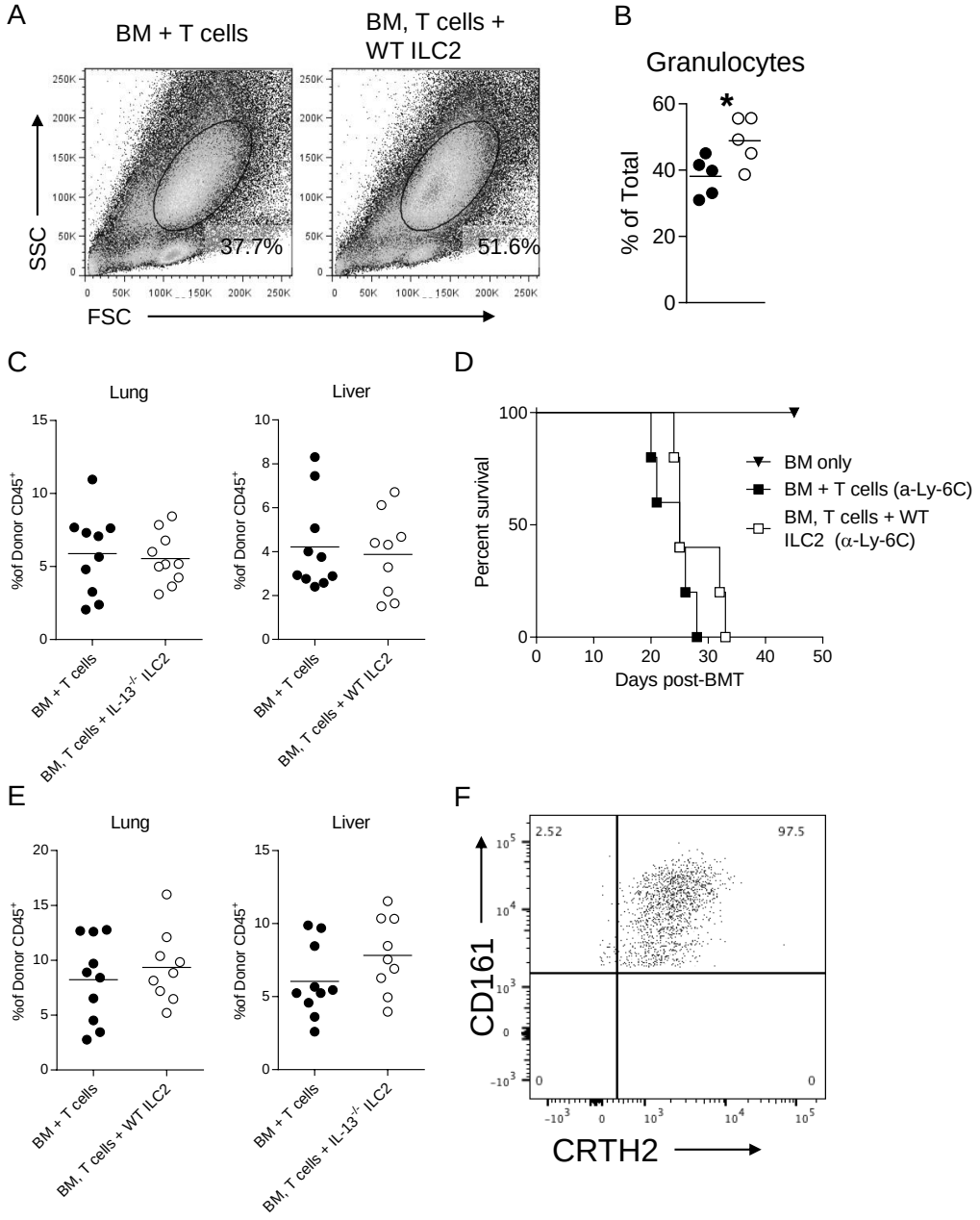

Supplemental Figure 6. MDSC evaluation and expansion of human ILC2s. (**A**) Density plots evaluating cells present in the colon on day 12 post-transplant. (**B**) Bar graph of mean ± SEM of granulocytes in the LP of BM + T cells (black dots) or BM, T cells + WT ILC2 (open circles) recipients. Representative of two experiments, (n=6), student's *t*-test with Welch's correction, * $p<0.05$. (**C**) Frequencies of MDSC in the lung and liver of allo-SCT recipients that received TCD BM + donor T cells +/- donor ILC2s, as described in (Fig. 4H) (**D**) Kaplan-Meier plot of Ly-6C depletion study, lethally irradiated B6D2 mice (950cGy) received 3.0 x 10^6 TCD BM (BM only), BM plus 4.0 x 10^6 total splenic T cells (BM + T cells) or BM plus T cells with 4.0 x 10^6 IL-33 activated ILC2s (BM, T

cells + WT ILC2) received 200µg anti-GR-1 (α-Ly-6C) twice weekly beginning 7 days post-transplant. One representative of 2 independent experiments shown, n=5 per group. (**E**) Frequencies of MDSC in the lung and liver as described (Fig. 5D). (**F**) Density plot of CD161 and CRTH2 expression on human ILC2 expanded from UCB after lineage depletion.

Supplemental Table 1

ILC2 Genes								ILC1/ILC3 Genes		
Gene	Counts	St. Dev.		Gene	Counts	St. Dev.			Counts	St. Dev.
Id2	21705.8	1863.1		Il1rl1 (ST2)	66607.9	7866.2		Tbx21	0.0	0.0
Gata3	16162.2	2308.3		Il17rb (IL-25R)	7929.7	2491.5		Ifng	2.4	1.4
Il5	67126.4	3853.0		Icos	17866.4	2702.8		Ncr1 (NKp46)	0.0	0.0
Il13	188515.9	14940.2		Klrg1	9179.0	1011.2		Rorc	1.8	1.6
Itga4	10949.6	3166.3		Areg	2248.6	301.7		IL17a	38.3	15.8
Itgb7	27193.7	4353.5						IL22	0.2	0.4

Table S1. Average read counts of innate lymphoid cell associated genes from RNA-seq of cultured ILC2 cells